Journal of Electrical and Electronic Engineering
2024; 12(1): 1-11
http://www.sciencepublishinggroup.com/j/jeee
doi: 10.11648/j.jeee.20241201.11
ISSN: 2329-1613 (Print); ISSN: 2329-1605 (Online)

Novel Control Approach for DC/DC Boost Converter Using Fuzzy Full State Feedback

Hajar Doubabi*, Mustapha El Adnani

School of Engineering and Innovation, Private University of Marrakesh (UPM), Marrakesh, Morocco

Email address:
h.doubabi@upm.ac.ma (Hajar Doubabi), m.eladnani@upm.ac.ma (Mustapha El Adnani)

*Corresponding author

To cite this article:
Hajar Doubabi, Mustapha El Adnani. (2024). Novel Control Approach for DC/DC Boost Converter Using Fuzzy Full State Feedback. *Journal of Electrical and Electronic Engineering*, *12*(1), 1-11. https://doi.org/10.11648/j.jeee.20241201.11

Received: December 26, 2023; **Accepted**: January 6, 2024; **Published**: January 18, 2024

Abstract: This paper presents a novel control strategy for output tracking in a DC/DC step-up converter, elevating the standard of precision and performance metrics. Beyond achieving commendable results, such as low Root Mean Square Error and rapid settling times, our novel approach ensures a seamless absence of overshoot, marking a significant advancement in both static and dynamic performance. A meticulous theoretical exploration forms the foundation of our proposed control methodology. Notably, our strategy excels through the integration of three pivotal factors: (i) a sophisticated small-signal model designed to operate seamlessly within the broad spectrum of the converter's operational range, (ii) the deployment of full-state feedback control, and (iii) the innovative incorporation of the Takagi-Sugeno fuzzy approach. Building upon a comprehensive understanding of the boost converter's topology, operational principles, and theoretical modeling, this paper delves into the intricacies of our suggested output control technique. The utilization of full-state feedback control and the Takagi-Sugeno fuzzy approach further reinforce the strategy's robustness, adaptability, and stability across diverse operating conditions. Simulations conducted in the Matlab/Simulink environment showcase the remarkable capabilities of our proposed control system, the precise reference tracking, resilience against input fluctuations and load disturbances, and unwavering compliance with performance requirements, our approach solidifies its status as a pioneering solution throughout the entire operational range of the system. In summary, our research not only introduces a state-of-the-art control approach but also underscores its effectiveness in achieving good static and dynamic performance metrics, thus contributing significantly to the advancement of DC/DC converter design.

Keywords: DC/DC Boost Converter, Full State Feedback Control, Takagi-Sugeno Fuzzy, Small Signal Modeling

1. Introduction

The Boost converter (BC) stands as an essential DC/DC converter, thanks to its various features that render it appropriate to be broadly employed in different industrial and power system applications that range from low-power handheld gadgets to high-power stationary ones. The BC topology, depicted in Figure 1, steps up the DC voltage from the input side to the output, by temporarily accumulating the supplied energy and transfer it to the load at an elevated level. The DC/DC BC is extensively used due to its limited number of components; this aspect is crucial when it comes to modeling, design, and fabrication [1].

However, from a control point of view, the nonlinear dynamic behavior is one of the major issues that the BC system faces. Therefore, it is necessary that the BC delivers a highly controlled DC output voltage under various system uncertainties, including the input voltage fluctuations and the load changes. In the literature, researchers have developed several control techniques for DC/DC converters, ranging from traditional methods to more advanced control approaches.

The traditional method as Proportional Integral Derivative (PID) control is widely used in the industrial processes due to its reduced complexity and its ease of implementation. However, despite its widespread usage, it exhibits poor performance. In reference [2], the authors designed a conventional PID controller specifically for controlling the boost converter output voltage. Based on simulation results, the PID controller demonstrated effective output voltage stabilization in the face of input voltage variations, but, it

suffered from significant overshoot and noticeable response time. In study [3], researchers introduced a fractional order PID controller as an alternative to the conventional one, aiming to achieve improved transient performance. The research papers [4, 5] have introduced a cascade controller based on an integral-proportional (IP) implemented for the outer-loop and a proportional-integral (PI) for the inner-loop to control a DC/DC boost converter. However, due to the inherent nonlinearity of this converter, the IP-PI cascade controller may not deliver the intended effectiveness in the presence of fluctuations in input voltage and parametric uncertainties.

In order to further enhance the performance, researchers have investigated different advanced and hybrid control techniques. In a previous study, a sliding mode controller is specifically designed for controlling the boost converter output voltage [6]. However, it exhibits variable switching frequency that presents difficulties in filter design and might introduce undesirable current harmonics. A two-loop controller that integrates super-twisting sliding-mode control with PI control was proposed and was validated through simulation and hardware studies in [7]. A dual loop controllers employing sliding mode and flatness controls was performed for a two cascade stages non-isolated DC/DC converter employed in fuel cell applications [8]. However, the need for prior knowledge regarding uncertainty bounds is still a major drawback of sliding mode control. To ensure global asymptotic stability of the closed-loop system, a nonlinear controller based on Lyapunov method was introduced in [9] and a backstepping controller using Lyapunov function was proposed in [10] for a DC/DC boost power converter. Although the controllers demonstrating satisfactory dynamic performance, their calculations and implementation are complex and challenging. The model predictive control was adopted to effectively driving the output voltage to the intended level and maintains its stability, even in the presence of destabilizing factors [11]. The controller performance was verified using experiments and simulations. However, this control strategy is susceptible to the influence of model inaccuracies, as it heavily depends on precise system models for accurate prediction and optimization. The application of metaheuristic methods has also been explored in the control of boost converters. A PSO-based algorithm that can directly regulate the output of the boost converter has been developed in [12]. Nevertheless, the lack of guarantee of optimality and the sensitivity to parameter settings are considered as major drawbacks of these methods. Moreover, several researchers have also dedicated their efforts to adopt the Fuzzy Logic Control (FLC) for DC/DC converter systems [13-15]. FLC has gained attention for its capacity to effectively control complex nonlinear systems with adaptability. Furthermore, various studies have illustrated how FLC can retain the advantageous features of classical control, such as feasibility and low computational complexity, while simultaneously enhancing its dynamic performance.

In the literature, a combination of FLC and PI is used to regulate a DC/DC converter [16-18]. The simulation and experimental findings reveal that this hybrid approach enhances the transient performance of the system. Additionally, these findings demonstrate that the Fuzzy-PI controller exhibits superior response compared to using Fuzzy or PI controllers individually. PI control is a conventional control technique primarily used for steady-state error correction, while state-feedback control is a more advanced approach that directly manipulates the internal states of the system for improved performance and stability. In the literature, the state-feedback control method has been proposed as a way to achieve a controller with high performance, offering advantages such as guaranteed robustness and superior disturbance compensation [19-22].

In this paper, a novel control strategy that combines FLC (Takagi–Sugeno (TS) type) and state-feedback control has been developed. The proposed strategy involves blending local state-feedback controllers by incorporating fuzzy membership functions resulting in the development of a global controller. Despite the inherent nonlinearity of the boost converter type, the proposed controller exhibits excellent control performance over the entire range of system operating points. The suggested method presents multiple benefits, encompassing the utilization of state-feedback controller advantages and the effective handling of nonlinearity through the FLC-TS, as well as simplified implementation with low computational cost due to the absence of complex mathematical computations. The proposed controller was subjected to simulation tests in the MATLAB/Simulink environment. The findings of the FLC-TS demonstrate improved flexibility, robustness, and the capacity to meet specifications across the whole interval of the converter operation.

The paper follows the following structure: Section 2 addresses the theoretical modeling of the boost converter. Section 3 provides a detailed explanation of the fuzzy full state feedback control strategy. Section 4 presents simulation outcomes that confirm the functionality of the controller. Finally, the conclusion is given in Section 5.

2. Boost Converter Modeling

The BC comprises various components, including DC power supply, an inductor, an electrical switch (Mosfet), a power diode, and an output capacitor. Figure 1 illustrates this configuration, with L and r_L representing the inductance and its internal resistance, C representing the capacitor, V_{in} representing the DC input voltage, V_{out} and i_{out} representing the output voltage and current of the boost converter, and i_L representing the electric current passing through the inductor.

For an optimal converter identification, the BC operating characteristics (output voltage versus duty cycle) is a useful curve for characterizing the converter operation and modeling its behavior. According to Table 1, the corresponding BC operating characteristics was plotted using Matlab/Simulink as illustrated in Figure 2. This curve demonstrates that the converter would stop boosting after a certain duty cycle. This is caused by the resistance ESR in the inductor and the power

switch, as well as the diode voltage drop, which set a maximum limit on the output voltage and duty cycle. In order to avoid control loop instability, it is crucial to set this limit for any practical BC.

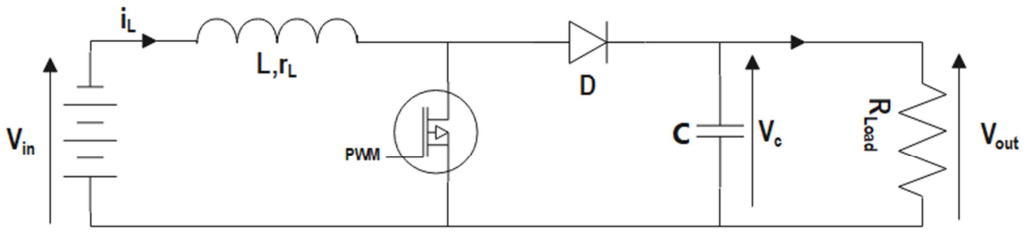

Figure 1. *DC/DC boost converter structure.*

Table 1. *DC/DC Boost converter.*

Parameter	Value	Unit
V_{in}	12	V
L, r_L	150, 8	µH, mΩ
C	470	µF
R_{Load}	70	Ω
f_s	30	kHz

f_s is the switching frequency. u is defined as the duty ratio piloting the power switches (diode and Mosfet).

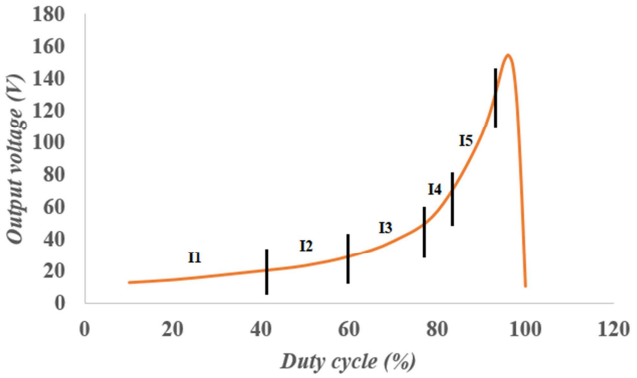

Figure 2. *BC operating curve divided into linear subintervals (I1 ...I5).*

As shown in Figure 2, it's evident that the BC demonstrates nonlinearity, introducing complexity into both modeling and control. Small signal linearization is among the most appropriate and straightforward approaches, which enables a precise model and accurate control. Its fundamental idea is to identify the system around specific operating points.

In this study, the operating curve of BC is firstly segmented into five linear subintervals [I1, I2, …, I5] (as depicted in Figure 2). Subsequently, state space models corresponding to each of these subintervals can be derived.

By applying Kirchhoff's current and voltage laws, we can derive the state space averaging model of the BC according to the two possible switch states.

$$\begin{cases} \dot{x} = A_i x + B_i E \\ y = C_i x \end{cases} \tag{1}$$

with $x = \begin{bmatrix} i_L \\ V_c \end{bmatrix}$, $E = L\dfrac{di_L}{dt}$

where i_L is the inductor current and V_c is the voltage across the capacitor.

$$A_1 = \begin{bmatrix} 0 & 0 \\ 0 & -\dfrac{1}{RC} \end{bmatrix} \quad B_1 = \begin{bmatrix} \dfrac{1}{L} \\ 0 \end{bmatrix} \quad C_1 = \begin{bmatrix} 0 & 1 \end{bmatrix}$$

$$A_2 = \begin{bmatrix} 0 & -\dfrac{1}{L} \\ \dfrac{1}{C} & -\dfrac{1}{RC} \end{bmatrix} \quad B_2 = \begin{bmatrix} \dfrac{1}{L} \\ 0 \end{bmatrix} \quad C_2 = \begin{bmatrix} 0 & 1 \end{bmatrix}$$

Where $i = 1$ for state 1 (switch is ON) and $i = 2$ for state 2 (switch is OFF).

2.1. State Space Average Model

The state space averaged model of the converter is presented by using the standard modeling approach for power electronic converters. Hence:

$$\begin{aligned} \dot{z} &= u\left(A_1 z + B_1 E\right) + \left(1-u\right)\left(A_2 z + B_2 E\right) \\ &= u\left(A_1 - A_2\right) z + A_2 z + B_2 E \end{aligned}$$

$$\begin{cases} \dot{z} = u\begin{bmatrix} 0 & \dfrac{1}{L} \\ -\dfrac{1}{C} & 0 \end{bmatrix} z + \begin{bmatrix} 0 & \dfrac{1}{L} \\ \dfrac{1}{C} & -\dfrac{1}{RC} \end{bmatrix} z + \begin{bmatrix} \dfrac{1}{L} \\ 0 \end{bmatrix} E \\ y_m = uC_1 z + \left(1-u\right) C_2 z \end{cases} \tag{2}$$

With $C_1 = C_2$, thus:

$$\begin{cases} \dot{z} = \begin{bmatrix} 0 & \dfrac{1}{L}(u-1) \\ \dfrac{1}{C}(1-u) & -\dfrac{1}{RC} \end{bmatrix} z + \begin{bmatrix} \dfrac{1}{L} \\ 0 \end{bmatrix} E \\ y_m = \begin{bmatrix} 0 & 1 \end{bmatrix} z \end{cases} \tag{3}$$

2.2. State Space Model Around an Equilibrium Point

The equilibrium point is generally defined under static operational conditions ($\dot{z} = 0$). The following system of algebraic equation can be utilized determine this point of equilibrium:

$$\begin{bmatrix} 0 & \frac{1}{L}(u_e-1) \\ \frac{1}{C}(1-u_e) & -\frac{1}{RC} \end{bmatrix} z_e + \begin{bmatrix} \frac{1}{L} \\ 0 \end{bmatrix} E = 0 \qquad (4)$$

yielding:

$$z_e = -\begin{bmatrix} 0 & \frac{1}{L}(u_e-1) \\ \frac{1}{C}(1-u_e) & -\frac{1}{RC} \end{bmatrix}^{-1} \begin{bmatrix} \frac{1}{L} \\ 0 \end{bmatrix} E$$

$$z_e = -\begin{bmatrix} \frac{-L}{R(1-u_e)^2} & \frac{C}{(1-u_e)} \\ \frac{-L}{(1-u_e)} & 0 \end{bmatrix} \begin{bmatrix} \frac{1}{L} \\ 0 \end{bmatrix}$$

$$z_e = \begin{bmatrix} \frac{-1}{R(1-u_e)^2} \\ \frac{-1}{(u_e-1)} \end{bmatrix} E \qquad (5)$$

Hence:

$$y_e = C_2 z_e$$

$$y_e = \frac{E}{u_e - 1} \qquad (6)$$

2.3. State Space Small Signal Model

Given that each variable can be described as a sum of a fixed component (static) and a small varying one (dynamic), as follows:

$$z = z_e + \hat{z}\ ;\ \ y_m = y_e + \hat{y}\ ;\ \ u = u_e + \hat{u}$$

The small signal model is obtained as follow:

$$\dot{z} = \dot{z}_e + \dot{\hat{z}}$$

$$\dot{z} = u(A_1 z + B_1 E) + (1-u)(A_2 z + B_2 E)$$

$$\dot{z}_e + \dot{\hat{z}} = (u_e + \hat{u})(A_1(z_e + \hat{z}) + B_1 E) + (1 - u_e - \hat{u})(A_2(z_e + \hat{z}) + B_2 E)$$
$$= u_e(A_1 z_e + B_1 E) + (1-u_e)(A_2 z_e + B_2 E) + u_e A_1 \hat{z} + \hat{u}(A_1 z_e + A_1 \hat{z} + B_1 E)(1-u_e) A_2 \hat{z} - \hat{u}(A_2 z_e + A_2 \hat{z} + B_2 E)$$

$$\dot{z}_e = u_e(A_1 z_e + B_1 E) + (1-u_e)(A_2 z_e + B_2 E)$$

$$\dot{\hat{z}} = u_e A_1 \hat{z} + \hat{u}(A_1 z_e + A_1 \hat{z} + B_1 E) + (1-u_e) A_2 \hat{z} - \hat{u}(A_2 z_e + A_2 \hat{z} + B_2 E)$$
$$= \hat{z}(u_e A_1 + (1-u_e) A_2) + (A_1 - A_2) z_e \hat{u} + (A_1 - A_2) \hat{u} \hat{z} + (B_1 - B_2) \hat{u} E$$

By neglecting the term $(A_1 - A_2)\hat{u}\hat{z}$, we obtain:

$$\dot{\hat{z}} = (u_e A_1 + (1-u_e) A_2) \hat{z} + (A_1 - A_2) z_e \hat{u} \qquad (7)$$

Hence

$$y_m = [0 \quad 1] z$$

$$y_e + \hat{y}_m = [0 \quad 1](z_e + \hat{z})$$

$$y_m = [0 \quad 1] \hat{z} \qquad (8)$$

3. Proposed Control Strategy

The aim of this section is to develop a robust controller that integrates full state feedback control with the Takagi-Sugeno (TS) fuzzy approach in order to for regulating the BC output voltage. The selection of the full state feedback control was based on its numerous benefits, including its strong robustness and its ability to provide superior compensation for disturbances. The choice of fuzzy logic was adopted to handle the converter nonlinearity.

Given a specific reference voltage $V_{in(ref)}$ (setpoint), the TS fuzzy controller generates a suitable duty cycle value, which define the BC operating point. And by using the small-signal model of BC, a full state feedback controller is synthetized for controlling the output voltage. Subsequently, for each operating point, a full state feedback control signal is derived to attain the output voltage control. In other words, the proposed strategy relies on effectively merging the state feedback controllers by means of fuzzy membership functions to attain a unified, global controller. This guarantee excellent control performance across the entire system operation range. The literature has explored the approach of linearization, which has demonstrated enhanced performance in numerous processes, namely three-level boost converter [17], micro

hydro power plant [23] and solar-gas dryer [18].

3.1. Full-State Feedback Control

Controllability is regarded as a fundamental and significant concept within the field of control systems. Hence, the system controllability must be firstly tested using the Kalman's test [24].

From Eq. (7) and (8), the obtained state equations of the small signal model are given as:

$$\begin{cases} \dot{\hat{z}} = [A]\hat{z} + [B]\hat{u} \\ \hat{y}_m = [C]\hat{z} \end{cases} \tag{9}$$

Where:

$$[A] = u_e A_1 + (1-u_e) A_2 = \begin{bmatrix} 0 & -\dfrac{1-u_e}{L} \\ \dfrac{1-u_e}{C} & -\dfrac{1}{RC} \end{bmatrix} \tag{10}$$

$$[B] = (A_1 - A_2) z_e = \begin{bmatrix} -\dfrac{E}{L(u_e-1)} \\ -\dfrac{E}{RC(1-u_e)^2} \end{bmatrix} \tag{11}$$

$$[C] = [0 \quad 1] \tag{12}$$

The matrix controllability is obtained as:

$$[\varphi] = [[B] \quad [A][B]] = \begin{bmatrix} -\dfrac{E}{L(u_e-1)} & \dfrac{E}{RLC(1-u_e)} \\ -\dfrac{E}{RC(1-u_e)^2} & \dfrac{E}{LC} + \dfrac{E}{(RC)^2(u_e-1)^2} \end{bmatrix} \tag{13}$$

Further:

$$\det[\varphi] = \frac{E^2\left(R^2C(u_e-1)^2 + 2L\right)}{L^2(RC)^2(1-u_e)^3} \tag{14}$$

$$\det[\varphi] = 5.45.10^{13} \neq 0$$

The determinant of the controllability matrix is non-zero. Hence, the rank is:

$$rank[\varphi] = 2 \tag{15}$$

As a result, the system is of controllable nature.

Full-state feedback describes a controller that follows a control-law like the one below to produce the input vector, u(t):

$$u(t) = [F] y_c(t) - [R] x(t) \tag{16}$$

Where $x(t)$is the state vector of the system, $y_c(t)$ is the desired state vector (setpoint), [R] is the controller gain matrix while [F] is the calibration matrix used to ensure a zero steady state error [25]. Figure 3 displays a schematic representation of the full state-feedback controller.

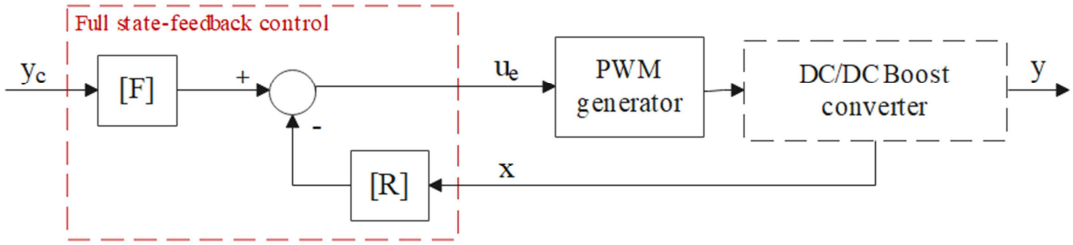

Figure 3. *Schema of the full state feedback controller.*

By synthetizing the appropriate matrices [R] and [F], one can opt for the desired system dynamics.

From (16), the full state feedback gain matrix is a row of vector of two unknown parameters given by:

$$[R] = [R1 \quad R2] \tag{17}$$

The closed-loop system behavior is contingent upon the eigenvalues and eigenvectors of the matrix [R]. The closed-loop poles are the eigenvalues of the closed-loop state dynamics matrix $([A]-[B][R])$, that are calculated as follow:

$$\det([A]-[B][R]-\lambda[I]) = (\lambda_1' - \lambda)(\lambda_2' - \lambda) \tag{18}$$

Thus,

$$\det[[A]-[B][R]-\lambda[I]] = \begin{vmatrix} \dfrac{R_1E}{L(u_e-1)} - \lambda & \dfrac{(u_e-1)}{L} - \dfrac{R_2E}{L(u_e-1)} \\ \dfrac{1-u_e}{C} + \dfrac{R_1E}{RC(1-u_e)^2} & -\dfrac{1}{RC} + \dfrac{R_2E}{RC(1-u_e)^2} - \lambda \end{vmatrix} \tag{19}$$

$$= \lambda^2 + \left(\frac{1}{RC} - \frac{R_2 E}{RC(1-u_e)^2} + \frac{R_1 E}{L(1-u_e)} \right) \lambda + \frac{R_1 E}{L(u_e - 1)} \left(\frac{1}{RC} - \frac{R_2 E}{RC(1-u_e)^2} \right) + \left(\frac{1-u_e}{L} + \frac{R_2 E}{L(1-u_e)} \right) \left(\frac{1-u_e}{L} + \frac{R_1 E}{L(1-u_e)^2} \right)$$

$$= \lambda^2 + \left(\frac{1}{RC} - \frac{R_2 E}{RC(1-u_e)^2} + \frac{R_1 E}{L(1-u_e)} \right) \lambda + \frac{2R_1 E}{RLC(1-u_e)} + \frac{(1-u_e)^2}{LC} + \frac{R_2 E}{LC}$$

$$= \lambda^2 - (\lambda_1' + \lambda_2') \lambda + \lambda_1' \lambda_2'$$

By identification, we obtain:

$$\begin{cases} \dfrac{1}{RC} - \dfrac{R_2 E}{RC(1-u_e)^2} + \dfrac{R_1 E}{L(1-u_e)} = -(\lambda_1' + \lambda_2') \\ \dfrac{2R_1 E}{RLC(1-u_e)} + \dfrac{(1-u_e)^2}{LC} + \dfrac{R_2 E}{LC} = \lambda_1' \lambda_2' \end{cases} \tag{20}$$

By solving Eq.24, we get the unknown parameters, R1 and R2, according to each given operating point u_e.

It is interesting to highlight that in this study; the closed-loop system is deliberately chosen to operate at five times the speed of the open-loop system. Consequently, λ_1' and λ_2' are given by:

$$\begin{cases} \lambda_1' = 5 \times \lambda_1 \\ \lambda_2' = 5 \times \lambda_2 \end{cases} \tag{21}$$

λ_1 and λ_2 are the eigenvalues of the matrix [A], which are computed as follow:

$$\det\left[[A] - \lambda [I] \right] = 0 \tag{22}$$

$$\det\left[[A] - \lambda [I] \right] = \lambda^2 + \frac{1}{RC} \lambda + \frac{(1-u_e)^2}{LC} = 0 \tag{23}$$

Depending on the given operating point u_e, the eigenvalues can be simply computed by solving Eq.23.

Finally, the matrix [F] can be calculated using Eq.24 as follow [24]:

$$[F] = \left[[C] \left[[B][R] - [A] \right]^{-1} [B] \right]^{-1} [G] \tag{24}$$

Where $[G] = [I]$ to achieve perfect accuracy and unit static transfer gain.

3.2. Takagi-Sugeno Fuzzy Approach

The linear full-state feedback controller described in section 3.1 can be created, but its optimal performance is guaranteed only when both the system state and input remain within the vicinity of the operating point. Therefore, we propose in this study, a novel control strategy that works by changing the full state feedback controller settings (the matrices [R] and [F]) in accordance with the given operating point. As seen in Figure 4, it can be described more simply as a multi-controller that uses a fuzzy logic-based selection algorithm. As a result, a global controller is developed to guarantee optimum performance over the system's whole operational range.

At a specified output voltage V_{out}, the configuration of the fuzzy system can be articulated as follows:

$$\text{Rule}^{\text{i}} : IF\, \overline{\text{V}}_{\text{out}} \in \text{I}_{\text{i}} THEN \left[R \right] \text{and} \left[F \right] \tag{25}$$

i=1, 2..., n; n is the fuzzy rules number, in this study *n=5*, and I_i is the i^{th} fuzzy set. The outputs of the fuzzy system can be characterized by utilizing a standard fuzzy inference technique that makes use of a singleton fuzzifier, product inference method, and weighted average defuzzifier:

$$\begin{cases} [\text{R}] = \left[\dfrac{\sum_{i=1}^{n} \mu_i(\overline{V}_{out}) \, \text{R}1_{\text{i}}}{\sum_{i=1}^{n} \mu_i(\overline{V}_{out})} \quad \dfrac{\sum_{i=1}^{n} \mu_i(\overline{V}_{out}) \, \text{R}2_{\text{i}}}{\sum_{i=1}^{n} \mu_i(\overline{V}_{out})} \right] \\ [\text{F}] = \left[\dfrac{\sum_{i=1}^{n} \mu_i(\overline{V}_{out}) \text{F}_{\text{i}}}{\sum_{i=1}^{n} \mu_i(\overline{V}_{out})} \right] \end{cases} \tag{26}$$

$\overline{V}_{out}$ represents the premise variable, μ denotes the normalized membership function and $\mu_i(\overline{V}_{out}) \Big/ \sum_{i=1}^{n} \mu_i(\overline{V}_{out}) \geq 0$ are the normalized weights.

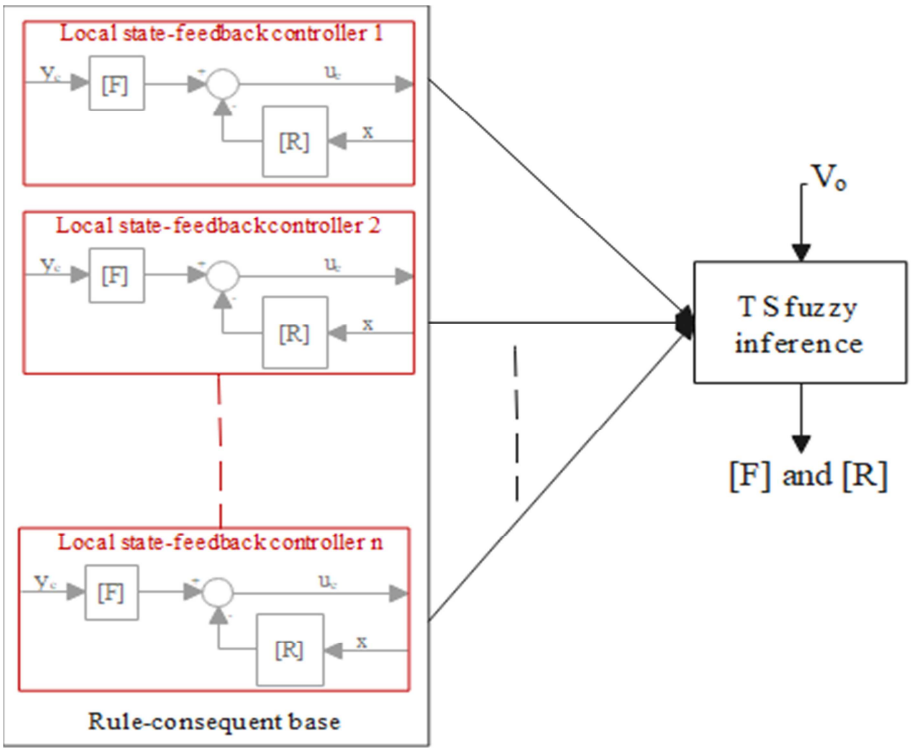

Figure 4. *The proposed TS fuzzy approach.*

As reported in Table 2, the proposed controller in this study determines the appropriate values for the matrices [R] and [F] corresponding to a specific BC output voltage. This is achieved by amalgamating the parameters of the synthetized full state feedback controller in a nonlinear manner, employing IF-THEN rules. The fuzzy system defines five linear subintervals [I1, I2... I5] as fuzzy sets, where I1 = [10-22], I2 = [22-31], I3 = [31-50], I4 = [50-71] and I5 = [71-132], encompassing the entire range of possibilities.

Figure 5 illustrates the selected membership functions for the fuzzy sets. The proposed control strategy anticipates the adequate matrices [R] and [F] that facilitate effective control using the Takagi–Sugeno Fuzzy approach.

Table 2. *Full state feedback parameters corresponding to each sub-interval.*

Sub-interval	Output voltage interval	Matrix [F]	Matrix [R]=[R1 R2]
I1	[10-22]Volt	[3.4067.10^-5]	[0.00524 -0.9]
I2	[22-31]Volt	[3.3934 10^-5]	[0.0006 -0.0208]
I3	[31-50]Volt	[3.39 10^-5]	[0.0005 -0.0133]
I4	[50-71]Volt	[3.3923 10^-5]	[0.0002 -0.0033]
I5	[71-132]Volt	[0.31]	[0.00153 0.04466]

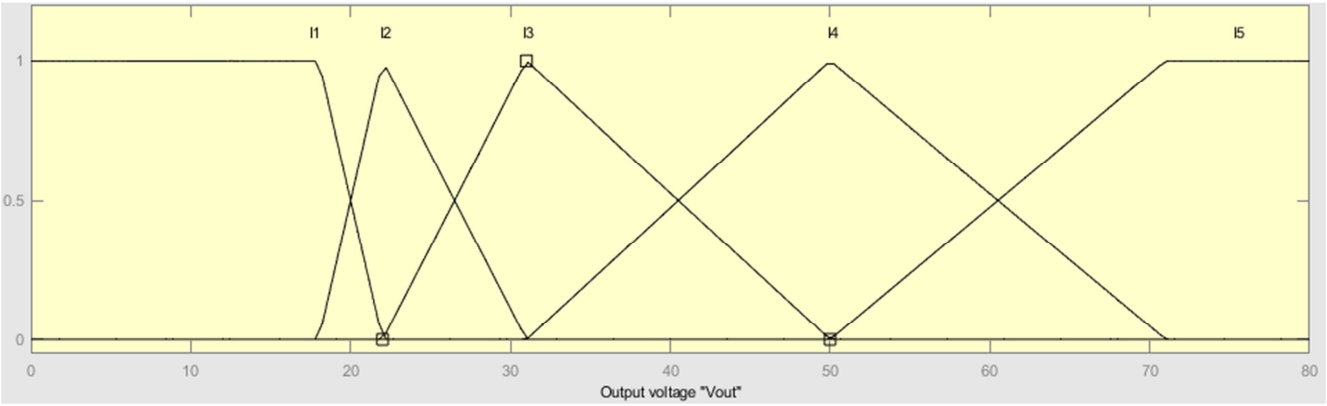

Figure 5. *Fuzzy set membership functions of the global controller.*

Considering the theorem of Wong et al. [26, 27], the stability of the closed-loop TSF control system is ensured

when specific criteria are met:

(i) It is necessary to ensure the local stability.

(ii) For the fuzzy logic inputs, complementary triangular membership functions must be used. (iii) The weighted average defuzzification method should be employed.

Since the local controllers in our scenario are built via the full state feedback method, their stability is guaranteed. This method is based on pole placement and typically defines the characteristic parameters necessary for creating a controller that ensures closed-loop stability [24]. These criteria were considered while synthetizing the design of the proposed controller, resulting in overall stability of the closed-loop system.

4. Simulation Results

In this part, the effectiveness of the proposed controller based on state feedback control and TS fuzzy approach has been validated through computer simulations using Matlab/Simulink environment. The numerical values of the power converter parameters employed in simulations are reported in Table 1. We are striving for a simulation that accurately reflects the real responses of the DC/DC boost converter circuit. Therefore, we took into consideration the non-ideal factors including switching and conduction losses in the power switches, reactive components and resistance losses in the transformer windings, by using the blocks of Simscape library.

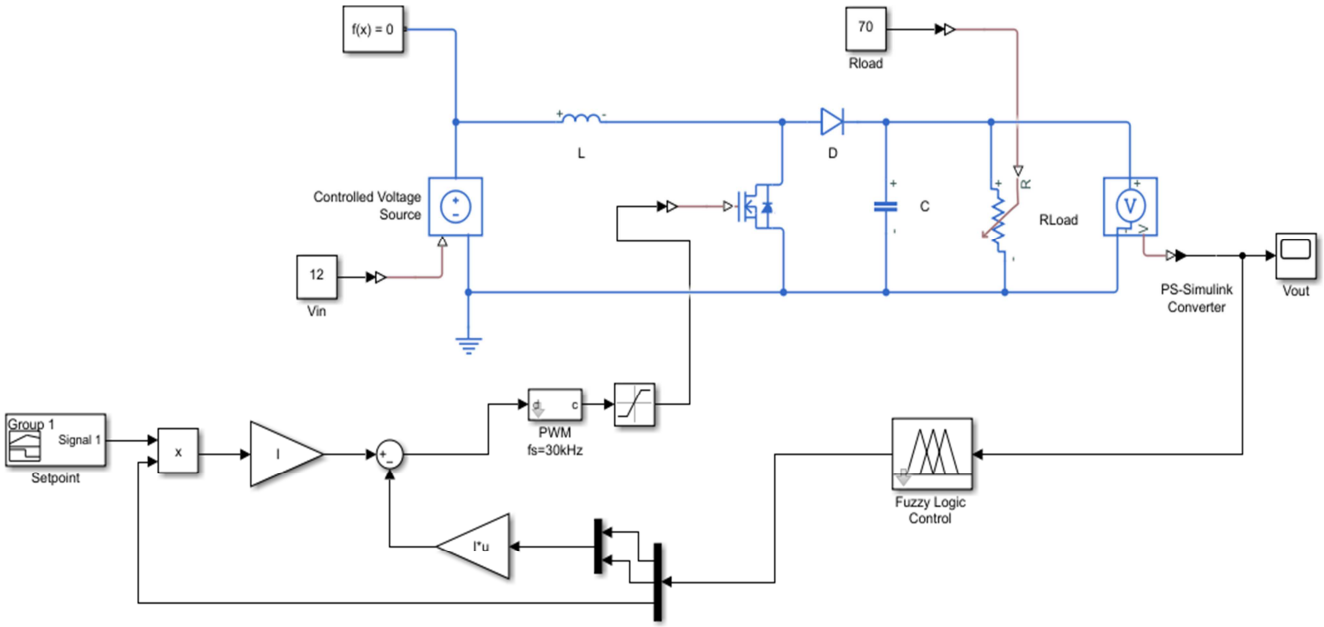

Figure 6. *Simulink model used for testing the proposed control of the DC/DC BC.*

The results of simulations are presented to bolster the theoretical analysis and highlight how successful the suggested control strategy is. Different scenarios were developed, focusing on assessing the performance of the proposed controller in response to set-point changes, input variations and load disturbances.

In the first scenario, findings from step changes in the reference voltage (setpoint) are presented in Figure 7. Specifically, the reference voltage is adjusted sequentially as follows: 15 V → 40 V → 25 V → 100 V → 60 V → 120 V → 10 V at time instances of 2s, 4s, 6s, 8s, 10s and 12s, respectively. This extended sequence was chosen to traverse various operating points within the five distinct linear intervals [I1, I2, …, I5], and the selected changes were deliberately set to cover both minor and significant variations.

Notably, the system output impeccably follows the reference (desired voltage) without exhibiting overshoot. The Root Mean Square Error (RMSE) has been plotted in Figure 8. is a widely adopted accuracy metric and it is defined by Eq.27. As can be seen, it remains in the range of 10^{-3}. This indicates that the controller rapidly adapts to the novel operating point. Additionally, the transient settling time, approximately 50ms, remains consistent irrespective of the direction of the setpoint step variation. This underscores the robustness of the suggested controller, demonstrating stability in both transient and steady-state behaviors when transitioning between operating points.

$$RMSE = \sqrt{\frac{1}{N}\sum_{k=1}^{N}\left(y_k - \hat{y}_k\right)^2} \tag{27}$$

where y represents the measured output, $\hat{y}$ is the target output, and the variable k ranges from 1 to N, is the total number of samples accessible for analysis.

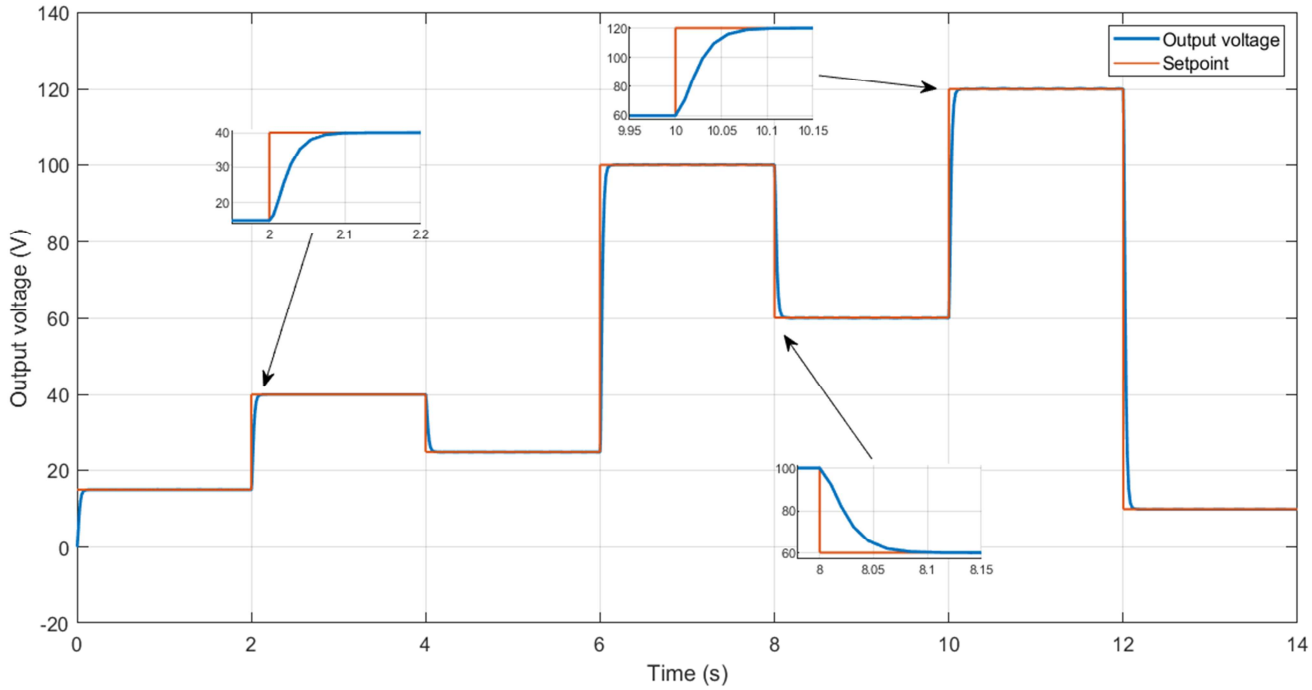

Figure 7. *Output voltage response to changes of set-points (actual vs. predicted curves).*

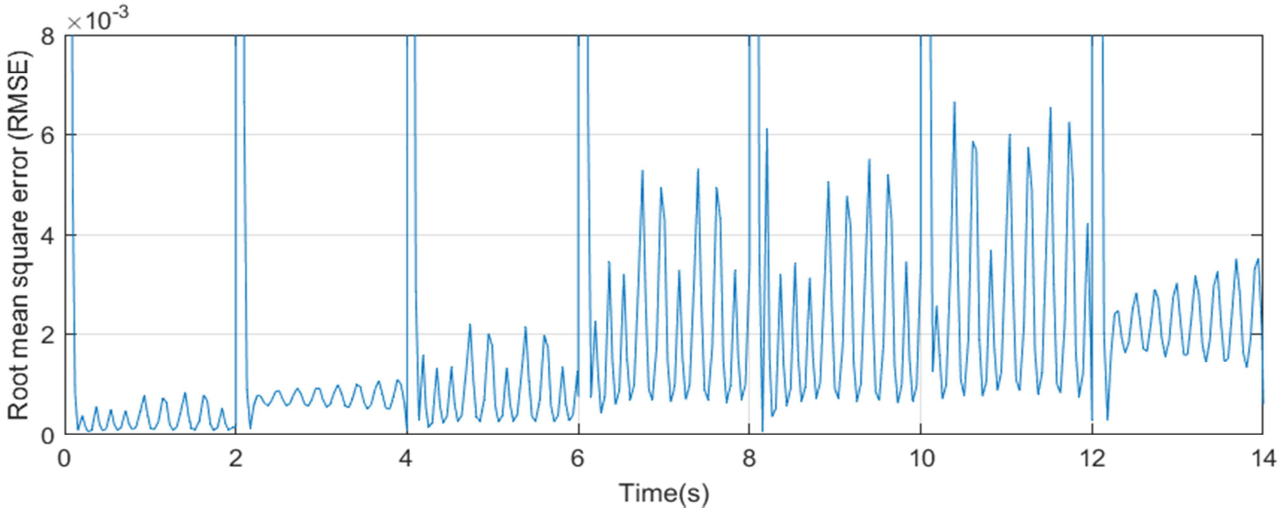

Figure 8. *Root mean square error.*

In the second scenario, the investigation focused on regulating the output voltage while subjecting it to load disturbances and input variations. The sequence for input voltage and load variation were designed as follows:

At t = 2 s, the load is adjusted from its nominal value, which is 70Ω, to 64Ω.

At t = 4.5 s, the load is adjusted from 64Ω to 112Ω.

At t = 7 s, the input voltage is varied from 12V to 14V.

At t = 9 s, the input voltage is changed from 14V to 10V.

Figure 9 displays the system's output voltage response. It's evident that, despite fluctuations in the load or input changes, the proposed controller enables the system to rapidly regain its stable state. This highlights the remarkable robustness of the proposed controller in the face of load disturbances and input fluctuations across the entire operational range.

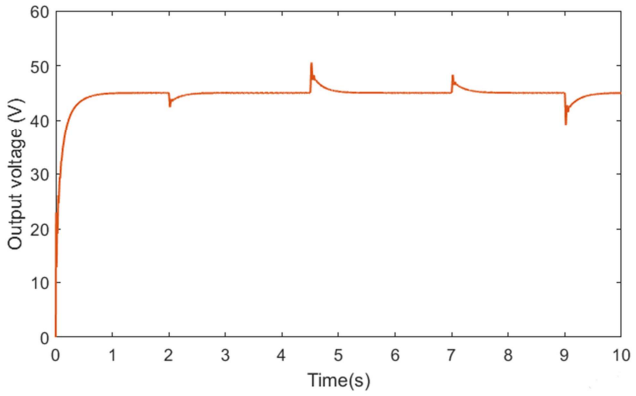

Figure 9. *Output voltage response in the presence of input variations and load disturbances.*

5. Conclusion

This research focuses on creating and implementing a robust output tracking controller for a DC/DC boost converter, combining Takagi-Sugeno fuzzy logic and full-state feedback control. The research begins with the synthesis of an accurate small-signal model. Then, the boost converter's operational characteristics is introduced to ensure precise prediction of the duty ratio for any desired output voltage. Subsequently, a local state-feedback control is investigated for output voltage regulation in the vicinity of specific operating points. Furthermore, the TS fuzzy approach is employed to design a versatile controller with robust adaptability across the entire operational range of the boost converter.

The proposed control algorithm is implemented using the MATLAB/Simulink environment, and various simulations are conducted to verify the viability of the proposed approach. The findings demonstrate that the boost converter's output voltage consistently tracks the setpoint from one step to another, characterized by low Root Mean Square Error (RMSE), very brief settling times, and no overshoot. This highlights the control strategy's ability to swiftly transition between operating points with both excellent static and dynamic performance. Additionally, the simulation findings underscore the controller's robustness in the face of input voltage variations and load fluctuations.

ORCID

https://orcid.org/0000-0003-0392-9854 (Hajar Doubabi)

Conflicts of Interest

The authors declare no conflicts of interest.

References

[1] M. Forouzesh, Y. P. Siwakoti, S. A. Gorji, F. Blaabjerg, and B. Lehman (2017). Step-up DC-DC converters: a comprehensive review of voltage-boosting techniques, topologies, and applications. IEEE Transactions on Power Electronics, vol. 32, no. 12, pp. 9143–9178.

[2] C. B. Ali, A. H. Khan, K. Pervez, T. M. Awan, A. Noorwali, and S. A. Shah (2021). High Efficiency High Gain DC-DC Boost Converter Using PID Controller for Photovoltaic Applications. 2021 International Congress of Advanced Technology and Engineering (ICOTEN). doi: 10.1109/icoten52080.2021.949.

[3] A. T. Mohamed, M. F. Mahmoud, R. A. Swief, L. A. Said, A. G. Radwan, (2021). Optimal fractional-order PI with DC-DC converter and PV system. Ain Shams Engineering Journal, 12(2), 1895–1906. doi: 10.1016/j.asej.2021.01.005.

[4] I. H. Kim and Y. I. Son (2015). Robust cascade control of DC/DC boost converter against input variation and parameter uncertainties. Proc. American Control Conf., Chicago, IL, USA, Jul. 1-3, pp. 2567–2572.

[5] I. H. Kim and Y. I. Son (2017). Regulation of a DC/DC Boost Converter Under Parametric Uncertainty and Input Voltage Variation Using Nested Reduced-Order PI Observers. IEEE Transactions on Industrial Electronics, 64(1), 552–562. doi: 10.1109/tie.2016.2606586.

[6] C. S. Sachin, S. G. Nayak, (2017). Design and simulation for sliding mode control in DC-DC boost converter. 2017 2nd International Conference on Communication and Electronics Systems (ICCES). doi: 10.1109/cesys.2017.8321317.

[7] M. F. Elmorshedy, S. Selvam, S. B. Mahajan, D. Almakhles (2023). Investigation of high-gain two-tier converter with PI and super-twisting sliding mode control. ISA Transactions, Vol. 138, pp. 628-638.

[8] R. Saadi, O. Kraa, M. Y. Ayad, M. Becherif, H. Ghodbane, M. Bahri, A. Aboubou (2016). Dual loop controllers using PI, sliding mode and flatness controls applied to low voltage converters for fuel cell applications. International Journal of Hydrogen Energy, 41(42), 19154–19163. doi: 10.1016/j.ijhydene.2016.08.171.

[9] Phattanasak, M., Gavagsaz-Ghoachani, R., Martin, J.-P., Pierfederici, S., Nahid-Mobarakeh, B., Riedinger, P. (2016). Lyapunov-based control and observer of a boost converter with LC input filter and stability analysis. 2016 International Conference on Electrical Systems for Aircraft, Railway, Ship Propulsion and Road Vehicles & International Transportation Electrification Conference (ESARS-ITEC). doi: 10.1109/esars-itec.2016.7841388.

[10] Boutebba, O., Semcheddine, S., Krim, F., & Talbi, B. (2019). Design of a Backstepping-Controlled Boost Converter for MPPT in PV Chains. 2019 International Conference on Advanced Electrical Engineering (ICAEE). doi: 10.1109/icaee47123.2019.9014748.

[11] Andres-Martinez, O., Flores-Tlacuahuac, A., Ruiz-Martinez, O. F., & Mayo-Maldonado, J. C. (2020). Nonlinear Model Predictive Stabilization of DC-DC Boost Converters with Constant Power Loads. IEEE Journal of Emerging and Selected Topics in Power Electronics, 1–1. doi: 10.1109/jestpe.2020.2964674.

[12] Fermeiro, J. B. L., Pombo, J. A. N., Calado, M. R. A., & Mariano, S. J. P. S. (2017). A new controller for DC-DC converters based on particle swarm optimization. Applied Soft Computing, 52, 418–434. doi: 10.1016/j.asoc.2016.10.025.

[13] Guo, L., Hung, J. Y., Nelms, R. M. (2012). Design of a fuzzy controller using variable structure approach for application to DC–DC converters. Electric Power Systems Research, 83(1), 104–109. doi: 10.1016/j.epsr.2011.09.005.

[14] Ganeswari, J. A., Kiranmayi, R. (2018). Performance improvement for DC boost converter with fuzzy controller. 2018 2nd International Conference on Inventive Systems and Control (ICISC). doi: 10.1109/icisc.2018.8399094.

[15] G. Ramesh, V. Ranjith Babu (2022). Comparative Study of PI and Fuzzy Control Strategies to A Novel Buck-Boost Converter. 2022 First International Conference on Electrical, Electronics, Information and Communication Technologies (ICEEICT). 10.1109/ICEEICT53079.2022.9768625.

[16] El Beid, S., Doubabi, S. (2014). DSP-Based Implementation of Fuzzy Output Tracking Control for a Boost Converter. IEEE Transactions on Industrial Electronics, 61(1), 196–209. doi: 10.1109/tie.2013.2242413.

[17] Doubabi, H., Salhi, I. (2021). Design and dSPACE Implementation of a Simplified Fuzzy Control of a DC-DC Three-Level Converter. Journal of Electrical and Computer Engineering, Vol. 2021, Article ID 5593572. https://doi.org/10.1155/2021/5593572

[18] Abdenouri, N., Zoukit, A., Salhi, I., Doubabi, S. (2022). Model identification and fuzzy control of the temperature inside an active hybrid solar indirect dryer. Solar energy, Vol. 231, 328-342. https://doi.org/10.1016/j.solener.2021.11.026.

[19] Ardhenta, L., Subroto, R. K. (2020). Feedback Control for Buck Converter - DC Motor Using Observer. 2020 12th International Conference on Electrical Engineering (ICEENG). doi: 10.1109/iceeng45378.2020.9171693.

[20] Olm, J. M., Fossas, E., Repecho, V., Doria-Cerezo, A., Grino, R. (2019). Feedback linearizing control of a magnetically coupled multiport dc-dc converter for automotive applications. IECON 2019 - 45th Annual Conference of the IEEE Industrial Electronics Society. doi: 10.1109/iecon.2019.8927831.

[21] P. Achikkulath, H. Shareef, R. Errouissi, A. Madathodika (2022). Feedback Linearizing Speed Control Strategy for Electric Vehicle Traction Motor drives. 2022 International Conference on Electrical and Computing Technologies and Applications (ICECTA). doi: 10.1109/ICECTA57148.2022.9990368.

[22] Rodriguez-Cabero, A., Prodanovic, M. none, Roldan, J. (2018). Full-State Feedback Control of Back-to-Back Converters Based on Differential and Common Power Concepts. IEEE Transactions on Industrial Electronics, 1–1. doi: 10.1109/tie.2018.2873518.

[23] I. Salhi, S. Doubabi, N. Essounbouli, A. Hamzaoui (2010). Application of multi-model control with fuzzy switching to a micro hydro-electrical power plant. Renewable Energy, Vol. 32, no. 12, pp. 9143–9178. doi: 10.1016/j.renene.2010.02.008.

[24] Hernández-Guzmán, V. M., Silva-Ortigoza, R. (2019). Book: Automatic Control with Experiments. Springer, Cham.

[25] Keviczky L. and al. Control engineering, Advanced Textbooks in Control and Signal Processing, Springer, 2019. https://doi.org/10.1007/978-981-10-8297-9

[26] Wong, L. K., Leung, F. H. F., Tam, P. K. S. (2001). A fuzzy sliding controller for nonlinear systems. IEEE Transactions on Industrial Electronics, 48(1), 32–37. doi: 10.1109/41.904545.

[27] Wong, L. K., Leung, F. H. F., Tam, P. K. S. (1998). Lyapunov-function-based design of fuzzy logic controllers and its application on combining controllers. IEEE Transactions on Industrial Electronics, 45(3), 502–509. doi: 10.1109/41.679009.